Nigerian Journal of Technology (NIJOTECH)
Vol. 45, No. 2, June 2026, pp. 1- 15
www.nijotech.com

Print ISSN: 0331-8443
Electronic ISSN: 2467-8821
https://doi.org/10.4314/njt.2026.5351

MODELING SHORT-CIRCUITING INDEX AS A CRITICAL MEASURE OF HYDRAULIC EFFICIENCY IN WASTE STABILIZATION POND

AUTHORS:
G. Ojo[1], *R. O. Onosakponome[2] and J. C. Agunwamba[1]

AFFILIATIONS:
[1]Department of Civil Engineering, University of Nigeria, Nsukka, NIGERIA
[2]Department of Civil Engineering, Federal University of Technology, Owerri, NIGERIA

***CORRESPONDING AUTHOR:**
Email: robertogaga2@gmail.com

ARTICLE HISTORY:
Received: July 25, 2025.
Revised: February 12, 2026.
Accepted: March 12, 2026.
Published: **Early view**

KEYWORDS:
Waste Stabilization Pond, Wastewater, Hydraulic efficiency, Short-circuiting, Treatment, Modeling.

ARTICLE INCLUDES:
Peer review

DATA AVAILABILITY:
On request from author(s)

EDITORS:
Chidozie Charles Nnaji

FUNDING:
None

Abstract

The simplest yet economical approach to municipal wastewater treatment is the utilization of Waste Stabilization Ponds (WSP). WSPs are relatively simple earthen basins that can be used to treat wastewater; their effectiveness depends on long detention periods and external elements like wind and sunlight. However, the presence of short-circuiting affects its hydraulic efficiency while minimization of short-circuiting will result in higher hydraulic efficiency. Consequently, in the study of WSP, short-circuiting is one of the most crucial factors that can be utilized as a gauge of its hydraulic efficiency. It is a more direct approach compared to other methods; hence, modeling short-circuiting index offers better assessment of its hydraulic performance. When some wastewater particles arrive at the pond's outlet before the anticipated detention time, this is known as short-circuiting. The model in this study was derived from the principle of conservation of mass, obtained by performing a mass balance analysis and solving the resulting two-dimensional equation numerically by the finite difference computational scheme, a scenario that is similar to the practical operation of a field WSP. The data used in the modeling were obtained from the literature of a lab-scale WSP experiment that incorporates short-circuiting index. The summary of the model results was as follows: for a flow of 58.8 ml/s, an average correlation coefficient of 92% and Root-Mean-Square-Error (RMSE) of 0.11 was recorded when compared with the experimental results. Similarly, an average correlation coefficient of 93.5% and RMSE estimate of 0.10 were obtained when the flow was 91.6 ml/s and for the flow of 120.8 ml/s; an average of 91.8% correlation were obtained with the average error of estimate of 0.13. The accuracy of the model in this study suggests a very good fit. It gave an overall average correlation of 92.4% with just 0.11 RMSE on the average. This result is reliable and the model is therefore recommended

HOW TO CITE:
Ojo, G., Onosakponome, R. O. and Agunwamba, J. C. "Modeling Short-Circuiting Index as a Critical Measure of Hydraulic Efficiency in Waste Stabilization Pond", *Nigerian Journal of Technology*, 2026. 45(2), pp. 1 – 15. https://doi.org/10.4314/njt.2026.5351

1.0 INTRODUCTION

The hydraulic behavior of waste stabilization ponds (WSPs), akin to other wastewater treatment systems, plays a critical role in determining mixing characteristics and overall treatment effectiveness [1]. Key factors influencing pond hydraulics include dead zones with minimal flow [10], the ratio of length to width [7], the strategic placement of inlet and outlet structures [8], the occurrence of short-circuiting, and the pond's depth [9]. Research has consistently shown that short-circuiting is a prevalent challenge in WSPs

[3]; [6]; [12]. Hydraulic efficiency is affected by phenomena such as eddy currents, surface flows, thermally induced vertical currents, density-driven currents, and the positioning of inlet and outlet structures. Poor placement of these structures can trigger short-circuiting, disrupting optimal flow patterns and diminishing hydraulic performance [6].

Optimal pond design, which considers both the pond's geometry and the relative positioning of its inlet and outlet, is essential for minimizing hydraulic short-circuiting [8]. According to [5], effective inlet structures should be economical, user-friendly, and designed to support sampling while reducing short-circuiting. For anaerobic and primary facultative ponds, inflows should be released below the water surface to limit scum formation, while secondary facultative and maturation ponds can discharge either above or below the water level. A single inlet and outlet, placed diagonally opposite each other at the pond's corners, are generally sufficient. Central inlet discharge should be avoided, as it increases the risk of short-circuiting. Complex configurations involving multiple inlets and outlets are neither necessary nor recommended. Outlets should be positioned to minimize scum discharge, with [8] recommending specific depths: 60 cm for facultative ponds, 30 cm for anaerobic ponds, and 5 cm for maturation ponds. To enhance WSP performance, designs must prioritize minimizing short-circuiting. The approach to forestall minimal or no occurrence of short-circuiting is vitally important and this is what constitute the main focus of this study. To achieve this basic objective of minimizing or eliminating short-circuiting, modeling short-circuiting index becomes necessary for the optimization of WSP hydraulic efficiency, an approach that is unique and differing from the other conventional methods. The other conventional methods includes incorporating baffles [7], [13] and maintaining a length-to-width ratio of at least 3.0 can significantly improve hydraulic efficiency by reducing short-circuiting. Additionally, optimizing pond geometry to achieve ideal dispersion conditions [14] enables more cost-effective construction of ponds, lagoons, and channels, especially for larger systems. This approach ensures that hydraulic and treatment processes are aligned with operational goals. Furthermore, regular monitoring and maintenance of inlet and outlet structures can prevent blockages and ensure consistent flow patterns, further enhancing the pond's treatment efficiency. By integrating these design principles, WSPs can achieve improved performance while maintaining cost-effectiveness and operational simplicity.

2.0 METHODOLOGY

The effective implementation of models for waste stabilization ponds (WSPs) demands a deeper understanding of mathematical methodologies. This research employed a computational strategy, solving the two-dimensional partial differential equation numerically through the finite difference method. Alongside other boundary conditions based on the pond's surface characteristics, the Danckwerts' boundary conditions [4] were applied. The 2-D finite difference approach was adopted in this study. Usually, short-circuiting often results from improper dispersion in the 2-D plains, viz; transverse and longitudinal dimensions of the pond and not likely from the vertical/depth dimension. Because the goal of transverse and longitudinal dispersion primarily is to carry wastewater molecules from the inlet to the outlet position of the pond, thereby resulting in short-circuiting in some cases, whereas, vertical dispersion mainly concerns with even mixing from the surface to the depth/bottom of the pond. As a result, the 2-D finite difference approach offers a more appropriate methodology compared to other existing methods.

2.1 Finite Difference Solution of the 2-D Equation

The general Equation (1) defines the behavior of internal nodes within the pond system. Depending on each node's position relative to boundary conditions, specific formulations—namely Equations (4) to (10), including (11) and (12) are applied within the grid to ensure accurate representation of physical processes and boundary interactions.

$$\frac{\partial c}{\partial t} = D_x \frac{\partial^2 c}{\partial x^2} + D_y \frac{\partial^2 c}{\partial y^2} - \frac{U\partial c}{\partial x} - \frac{V\partial c}{\partial y} - \mathrm{Kc} \qquad (1)$$

Writing the finite difference scheme

https://doi.org/10.4314/njt.2026.5351

$\frac{\partial C}{\partial t} = \frac{C_{i+1,j}-C_{i-1,j}}{2t} \frac{\partial^2 C}{\partial x^2} = \frac{C_{i+1,j}-2C_{i,j}+C_{i-1,j}}{h^2} \frac{\partial^2 C}{\partial y^2} = \frac{C_{i,j+1}-2C_{i,j}+C_{i,j-1}}{p^2} \frac{\partial C}{\partial x} = \frac{C_{i+1,j}-C_{i-1,j}}{2h} \frac{\partial C}{\partial y} = \frac{C_{i,j+1}-C_{i,j-1}}{2p} \frac{C_{i+1,j}-C_{i-1,j}}{2t} = Dx\left[\frac{C_{i+1,j}-2C_{i,j}+C_{i-1,j}}{h^2}\right] + Dy\left[\frac{C_{i,j+1}-2C_{i,j}+C_{i,j-1}}{p^2}\right] - U\left[\frac{C_{i+1,j}-C_{i-1,j}}{2h}\right] - V\left[\frac{C_{i,j+1}-C_{i,j-1}}{2p}\right] - KC_{i,j} \frac{C_{i+1,j}-C_{i-1,j}}{2t} = \left(\frac{Dx}{h^2}+\frac{U}{2h}\right)C_{i+1,j} + \left(\frac{Dx}{h^2}+\frac{U}{2h}\right)C_{i-1,j} + \left(\frac{Dy}{p^2}-\frac{V}{2p}\right)C_{i,j+1} + \left(\frac{Dy}{p^2}+\frac{V}{2p}\right)C_{i,j-1} - (\frac{2Dx}{h^2}+\frac{2Dy}{p^2}+K)\,C_{i,j}$ (2)

Boundary and initial conditions

$UC_{in} = UC_o - D\frac{\partial C}{\partial x}, x = 0$ (Inlets)

$\frac{\partial C}{\partial x}$ =0, x = 0, 0<y<B

$\frac{\partial C}{\partial x} = 0,\ x = L$ (Outlet end)

$\frac{\partial C}{\partial x}$ = 0, y=0, B

$\frac{\partial C}{\partial t}$ =0, t=0, x=0

$\frac{\partial C}{\partial t}$ =0, t=t, x=L

At the inlet where x = 0, the term $C_{i-1,j}$ outside the scheme was obtained

$\frac{C_{i+1,j}-C_{i-1,j}}{2t} = (\frac{Dx}{h^2}+\frac{U}{2h})\ C_{i+1,j} + (\frac{Dx}{h^2}+\frac{U}{2h})\ C_{i-1,j} + (\frac{Dy}{p^2}-\frac{V}{2p})\ C_{i,j+1} + (\frac{Dy}{p^2}+\frac{V}{2p})C_{i,j-1} - (\frac{2Dx}{h^2}+\frac{2Dy}{p^2}+K)\ C_0$ (3)

By invoking the boundary condition for the inlet;

$$UC_{in} = UC_o - D\frac{\partial C}{\partial x}$$

A finite difference approximation can replace the derivative, with Co denoting the concentration at the inlet location, where x equals zero.

$$C_{in} = UC_o - Dx\left(\frac{C_{i+1,j}-C_{i-1,j}}{2h}\right)$$

which can be solved to give,

$$C_{i-1,j} = \frac{2hu}{Dx}C_{in} - \frac{2hu}{Dx}C_o + C_{i+1,j}$$

Substitute in Equation (3)

$\left(\frac{2Dx}{h^2}+\frac{2Dy}{p^2}+K+\frac{2U}{h}+\frac{U^2}{Dx}\right)C_o - \left(\frac{2Dx}{h^2}\right)C_{i+1,j} - \left(\frac{Dy}{p^2}+\frac{V}{2p}\right)C_{i,j-1}\left(\frac{Dy}{p^2}-\frac{V}{2p}\right)C_{i,j+1} = \left(\frac{2U}{h}+\frac{U^2}{Dx}\right)C_{in}$ (4)

$$\frac{\partial C}{\partial x} = 0, \quad x = 0, \quad 0 < y < B$$

$$\frac{C_{i+1,j}-C_{i-1,j}}{2h} = 0$$

It implies that, $C_{i+1,j} = C_{i-1,j}$, Substitute in equation (2)

$\frac{C_{i+1,j}-C_{i-1,j}}{2t} = \left(\frac{2Dx}{h^2}\right)C_{i+1,j} + \left(\frac{Dy}{p^2}-\frac{V}{2p}\right)C_{i,j+1} + \left(\frac{Dy}{p^2}+\frac{V}{2p}\right)C_{i,j-1} - (\frac{2Dx}{h^2}+\frac{2Dy}{p^2}+K)\ C_{i,j}$ (5)

At the edge of the pond where x = 0, y = 0

$$\frac{\partial C}{\partial x} = 0$$

$$\frac{C_{i,j+1}-C_{i,j-1}}{2p} = 0$$

Hence $C_{i,j+1} = C_{i,j-1}$, substitute in equation (5)

$\frac{C_{i+1,j}-C_{i-1,j}}{2t} = \left(\frac{2Dx}{h^2}\right)C_{i+1,j} + \left(\frac{2Dy}{p^2}\right)C_{i,j-1} - (\frac{2Dx}{h^2}+\frac{2Dy}{p^2}+K)C_{i,j}$ (6)

At the edge of the pond where x = 0, y = B

$\frac{C_{i+1,j}-C_{i-1,j}}{2t} = \left(\frac{2Dx}{h^2}\right)C_{i+1,j} + \left(\frac{2Dy}{p^2}\right)C_{i,j-1} - (\frac{2Dx}{h^2}+\frac{2Dy}{p^2}+K)$ (7)

For the outlet, the slope must be zero, that is;

$$\frac{\partial C}{\partial x} = 0, \quad x = L, \quad 0 < y < B$$

https://doi.org/10.4314/njt.2026.5351

The finite divided difference will yield, $C_{i+1,j} = C_{i-1,j}$, substitute in equation (2)

$$\frac{C_{i+1,j}-C_{i-1,j}}{2t} = \left(\frac{2Dx}{h^2}\right) C_{i-1,j} + \left(\frac{Dy}{p^2} - \frac{V}{2p}\right) C_{i,j+1} + \left(\frac{Dy}{p^2} + \frac{V}{2p}\right) C_{i,j-1} - \left(\frac{2Dx}{h^2} + \frac{2Dy}{p^2} + K\right) C_{i,j} \quad (8)$$

At the pond outlet ends, for which y = 0, the equation can be written as

$$\frac{C_{i+1,j}-C_{i-1,j}}{2t} = \left(\frac{2Dx}{h^2}\right) C_{i-1,j} + \left(\frac{2Dy}{p^2}\right) C_{i,j+1} - \left(\frac{2Dx}{h^2} + \frac{2Dy}{p^2} + K\right) C_{i,j} \quad (9)$$

At the pond outlet ends for which y = B, the equation becomes

$$\frac{C_{i+1,j}-C_{i-1,j}}{2t} = \left(\frac{2Dx}{h^2}\right) C_{i-1,j} + \left(\frac{2Dy}{p^2}\right) C_{i,j-1} - \left(\frac{2Dx}{h^2} + \frac{2Dy}{p^2} + K\right) C_{i,j} \quad (10)$$

At the sides of the pond,

$$\frac{\partial C}{\partial x} = 0, \qquad y = 0, B$$

It implies as before $C_{i,j+1} = C_{i,j-1}$, substitute in equation (2) for y = 0

$$\frac{C_{i+1,j}-C_{i-1,j}}{2t} = \left(\frac{Dx}{h^2} + \frac{U}{2h}\right) C_{i+1,j} + \left(\frac{Dx}{h^2} + \frac{U}{2h}\right) C_{i-1,j} + \left(\frac{2Dy}{p^2}\right) C_{i,j+1} - \left(\frac{2Dx}{h^2} + \frac{2Dy}{p^2} + K\right) C_{i,j} \quad (11)$$

For y = B

$$\frac{C_{i+1,j}-C_{i-1,j}}{2t} = \left(\frac{Dx}{h^2} - \frac{U}{2h}\right) C_{i+1,j} + \left(\frac{Dx}{h^2} + \frac{U}{2h}\right) C_{i-1,j} + \left(\frac{2Dy}{p^2}\right) C_{i,j-1} - \left(\frac{2Dx}{h^2} + \frac{2Dy}{p^2} + K\right) C_{i,j} \quad (12)$$

2.2 Software Application

Solving systems involving multiple partial differential equations often requires advanced computational tools due to the complexity and volume of numerical calculations. In this study, MATLAB was employed as the primary computational platform to address these challenges. Renowned for its efficiency in numerical computing, MATLAB offers a robust environment for handling complex mathematical models, enabling researchers to perform iterative computations, data visualization, and algorithm development with relative ease [11]. Its comprehensive library of built-in functions supports various tasks such as matrix operations, differential equation solving, and graphical rendering. Moreover, the software's high-level programming language allows for seamless customization and the integration of user-defined scripts, making it particularly suitable for simulating and analyzing engineering systems governed by partial differential equations.

2.3 Grid development

To accurately simulate a waste stabilization pond, it is important to use a tiny grid with modest entry and exit points. Increasing grid density typically improves solution accuracy. A flow chart summarizing the entire modeling process is shown in Figure 1 below.

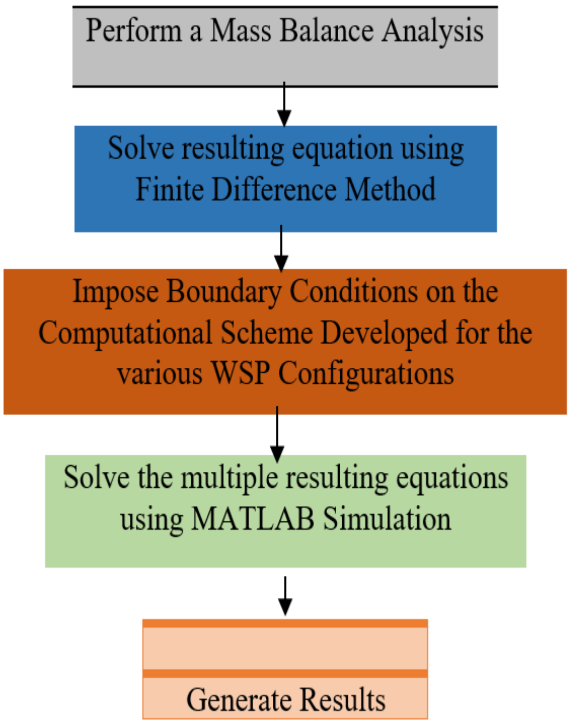

Figure 1: A simple flow diagram summarizing the modeling steps for easy comprehension.

2.4 Review of the Experimental Setup for the Modeling Purpose

This study employed experimental data from the literature [2], Reynolds model similarity law was applied to take care of scale effect and other discrepancies in the experimental processes. Figure 2 depicts the experimental setup for studying how inlet and outlet structures affect

https://doi.org/10.4314/njt.2026.5351

short-circuiting. The system incorporates a reservoir that receives constant water supply from a channel via a pump and pipe. Pumping at a regular rate ensures consistent reservoir water level throughout trials. The reservoir delivers water to three ponds (channels) with lengths of 1.0, 1.5, and 2 meters. Each pond has a cross-section of 0.5m x 0.4m. Each pond has three inlets and three exits, as illustrated in Figure 2. When one set of inlet-outlet position is open, the rest remain closed [2].

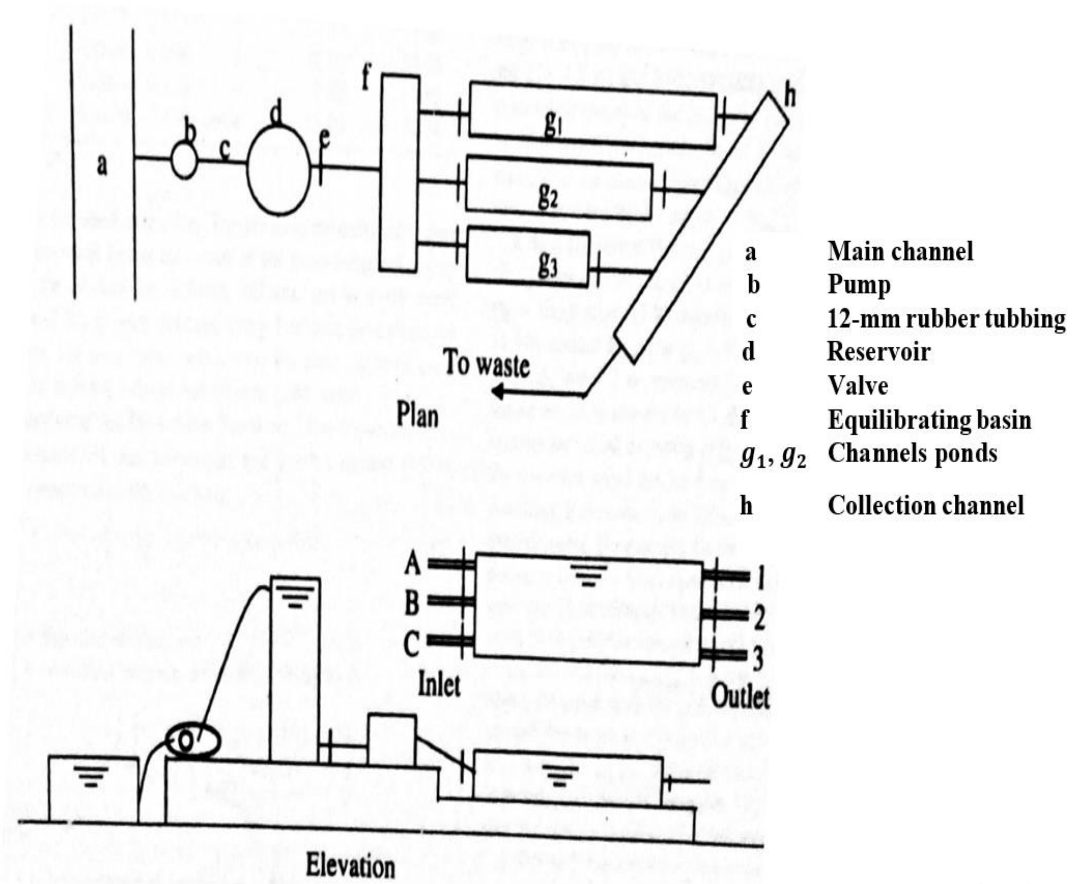

source: [2]

Figure 2: Experimental setup.

2.5 Calculation of the Short-circuiting Index

The short-circuiting index (α) was determined analytically using Equation (13) below. The theoretical detention time was calculated as shown in equation (14) while the actual detention time were obtained from the experiment using the effluent concentration (C_e) at the outlet of the pond.

$$\alpha = 1 - \frac{\theta_a}{\theta_t} \tag{13}$$

θ_a= actual detention time (minutes)

$\theta_t = \frac{V}{Q}$, the theoretical detention time (14)

3.0 RESULTS AND DISCUSSION

3.1 Convergence and Stability of the Finite Difference Solutions

Convergence means that as Δx, Δy and Δz approached zero, the results of the finite difference technique approach the true solution. Stability on the other hand means that errors at any stage of the computation are not amplified but are attenuated as the computation progresses. Also, static instability may result when the computation is subjected to numerical errors. The criterions used to avoid this static instability are shown in Equation 15 below.

$$\Delta x \le \frac{2Dx}{u}, \Delta y \le \frac{2Dy}{v} \text{ and } \Delta z \le \frac{2Dz}{w} \tag{15}$$

Where, Δx, Δy and Δz are the mesh sizes in the x, y and z coordinates respectively, Dx, Dy and Dz are the coefficients of dispersion in x, y and z coordinates respectively, while u, v and w are the fluid velocities in x, y and z coordinates respectively. If criterion is not satisfied, then Δx, Δy and Δz must be lowered. For all cases computed, the criterion was satisfied.

For convergence test, the numerical solution (C_x) must approach the analytic solution (C) as Δx, Δy and Δz tends to zero. Hence, $C - C_x$ is equal to disretization error (truncation error) and it is dependent both on the accuracy of the scheme and the grid spacing. The finite difference solution converged for all the computations.

3.2 Model Results

3.2.1 BOD Removal Efficiency

Figure 3 below shows the model result of the pond configuration with the various gridlines representing the actual flow lines in the pond. The result demonstrates the actual condition of the pond during operation.The plot shows the variation in the concentration values from the inlet section of the pond to the outlet, significantly indicating the BOD removal efficiency. The decreasing BOD concentration varies from the inlet and gradually converges towards the outlet point where the wastewater could be said to have been stabilized with a significant amount of BOD remove

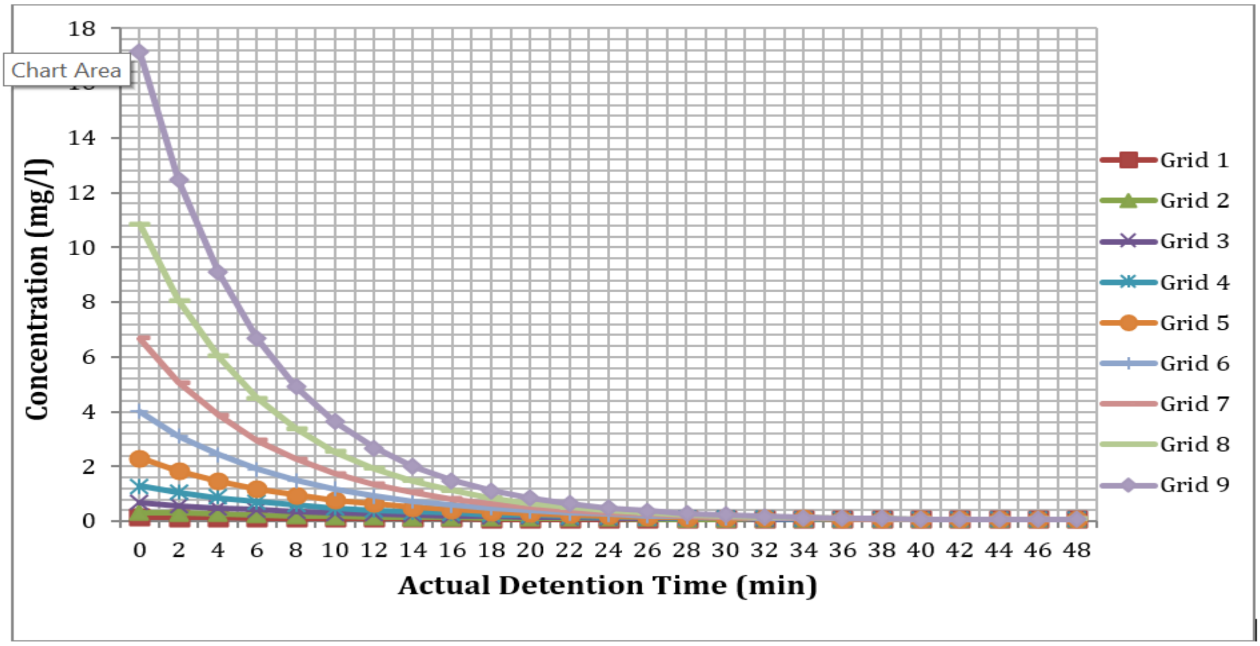

Figure 3: Concentration-time graph showing the model result of the pond with the grid representing the flow lines

3.2.2 Determination of the Short-circuiting Index

The modeled variation of concentration for the pond configuration A3, that is, the pond with inlet A and outlet 3 is presented in Table 1 below. These results varies with the pond geometry for (L = 1.0, 1.5 and 2.0 m) as well as the influent flow rate (Q = 58.8, 91.6 and 120.8 ml/s).

Table 1 shows the actual detention time with its corresponding effluent concentration within the pond. The concentration-time curve for configuration A3 was obtained as shown in Figure 4 below. The actual detention time using the effluent concentration was determined for the purpose of estimating the short-circuiting index.

https://doi.org/10.4314/njt.2026.5351

Table 1: Model results for inlet and outlet configuration A3 corresponding to grid 1 for pond length, L = 2.0 m with an influent flow rate, Q = 58.8 ml/s

Time				Effluent	Concent ration	(mg/l)			
(min)	Grid 1	Grid 2	Grid 3	Grid 4	Grid 5	Grid 6	Grid 7	Grid 8	Grid 9
0	0.148623	0.327653	0.66912	1.276836	2.308342	3.996362	6.677953	10.83328	17.1366
2	0.137278	0.288455	0.566955	1.047483	1.840659	3.106029	5.069509	8.046163	12.46963
4	0.12711	0.254716	0.481921	0.862128	1.472574	2.422088	3.861373	5.996235	9.10435
6	0.117989	0.225623	0.410985	0.711945	1.182084	1.895192	2.951249	4.483978	6.670287
8	0.109801	0.200493	0.351676	0.589953	0.952204	1.48812	2.263596	3.364989	4.904336
10	0.102446	0.178752	0.301982	0.490611	0.769794	1.172719	1.74249	2.534471	3.619124
12	0.095837	0.159916	0.26026	0.409518	0.624663	0.927647	1.346415	1.91616	2.680837
14	0.089898	0.143576	0.225162	0.343164	0.508884	0.736677	1.044469	1.454408	1.99365
16	0.084562	0.129388	0.195584	0.288747	0.416282	0.587445	0.813592	1.108497	1.488747
18	0.079771	0.117059	0.170618	0.244025	0.342029	0.470504	0.636531	0.848556	1.116572
20	0.075474	0.106341	0.149519	0.207198	0.282348	0.378617	0.50034	0.652606	0.841338
22	0.071625	0.097025	0.13167	0.176821	0.234272	0.306228	0.395283	0.504436	0.63713
24	0.068186	0.088933	0.116562	0.151731	0.195469	0.249063	0.314018	0.392057	0.485129
26	0.065123	0.081912	0.103777	0.13099	0.164101	0.203824	0.250998	0.306577	0.37163
28	0.062405	0.075836	0.092966	0.113841	0.138718	0.167962	0.202017	0.241385	0.28663
30	0.060006	0.070595	0.083843	0.099674	0.118173	0.139505	0.163884	0.191557	0.222803
32	0.057904	0.066098	0.076172	0.087994	0.10156	0.116924	0.134173	0.153417	0.174779
34	0.05608	0.062268	0.069758	0.078405	0.088164	0.099035	0.111039	0.124215	0.138611
36	0.054516	0.059041	0.064442	0.070588	0.077422	0.084921	0.093078	0.101899	0.111395
38	0.0532	0.056363	0.060094	0.064288	0.068891	0.073875	0.079226	0.084936	0.091001
40	0.052119	0.054191	0.056612	0.059304	0.062228	0.065359	0.068682	0.072188	0.075869
42	0.051265	0.052492	0.053914	0.055483	0.057172	0.058965	0.060851	0.062822	0.064873
44	0.05063	0.051238	0.051938	0.052707	0.053529	0.054396	0.055303	0.056244	0.057216
46	0.05021	0.050411	0.050643	0.050896	0.051166	0.051449	0.051745	0.05205	0.052364
48	0.05021	0.050411	0.050643	0.050896	0.051166	0.051449	0.051745	0.05205	0.052364

https://doi.org/10.4314/njt.2026.5351

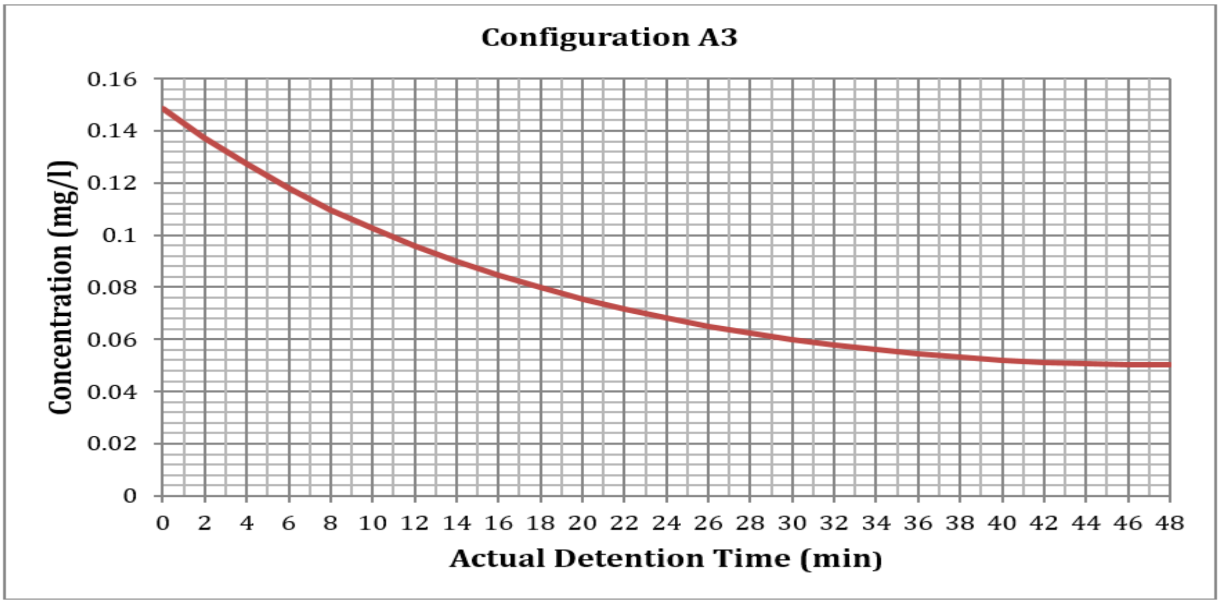

Figure 4: Concentration – time curve for configuration A3, pond length, L = 2.0 m at influent flow rate, Q = 58.8 ml/s

The concentration – time curve presented in Figure 4 above shows that for ;C_e value of 0.052 mg/l, the predicted actual detention time, $\theta_a$was 46.00 min (Experimental θ_a was found to be 46.482 min). The theoretical detention time, θ_t *was determined to be* 56.59 *min*, therefore; Short-circuiting index, α *is equal to* 0.19 (using Equation 2)

Experimental Short-circuiting index, $\alpha = 0.18$

The result shows a good correlation of 96% between the experimental and modeled short-circuiting index, only with an insignificant Root Mean Square Error (RMSE) of 0.06. The correlation and RMSE values are statistical measures of evaluation of the model performance. A higher correlation value implies a degree of good fit, how well the model defines or predict the practical wastewater treatment efficiency. However, a very low RMSE value implies a high degree of the model performance. The real-world application demonstrates how well the model can be used in providing honest assessment of WSP hydraulic efficiency, so as to propose its optimization where necessary. The model does not only show a good fit with the index but also for the varying effluent concentration within the pond. This result when compared with [15], shows the effectiveness of the 2-D model compared to the 3-D CFD model as far as short-circuiting is concerned.

Table 2 presents the results for configuration C3 obtained by simulating for pond, L = 1.0 m with an inflow rate of 91.6 ml/s. The concentration-time curve is presented in figure 5; this is corresponding to grid 4 with respect to the computational scheme. The same performance trend with respect to the model was also observed, the changes in pond length and inflow rate notwithstanding. Although, there is a significant decrease in the pond hydraulic efficiency with an index of 0.19 for A3 above compared to 0.34 in C3. This is due to the higher length to width ration (l/w) and a lower flow rate of the former. The SCI values depend on a number of factors like pond geometry, the influent flowrate as well as the configuration of the inlet and outlet structures. For this study, the results varies with the pond geometry for (L = 1.0, 1.5 and 2.0 m) as well as the influent flow rate (Q = 58.8, 91.6 and 120.8 ml/s). For instance, for configuration A3, pond length, L = 2.0 m at influent flow rate, Q = 58.8 ml/s yields a better result with SCI value of 0.18. This is so, because the factors responsible for short-circuiting to take place has not been very favored, namely; lowest flowrates, largest pond length and the widest staggered inlet/outlet configuration.

https://doi.org/10.4314/njt.2026.5351

Table 2: Model results for inlet and outlet configuration C3 corresponding to grid 4 for pond length, L = 1.0 m with an influent flow rate, Q = 91.6 ml/s

Time				Effluent	Concent rated	(mg/l)			
(min)	**Grid 1**	**Grid 2**	**Grid 3**	**Grid 4**	**Grid 5**	**Grid 6**	**Grid 7**	**Grid 8**	**Grid 9**
0	0.290338	0.50589	0.874865	1.474941	2.419184	3.867652	6.043198	9.252108	13.91065
1	0.258089	0.431926	0.720833	1.177875	1.878828	2.928746	4.470938	6.698547	9.869207
2	0.229187	0.36888	0.594502	0.941925	1.461509	2.221686	3.313973	4.859362	7.016301
3	0.20326	0.315058	0.490712	0.75418	1.138606	1.688187	2.460902	3.531977	4.998164
4	0.179985	0.269044	0.405302	0.604531	0.888301	1.28488	1.830666	2.572034	3.567582
5	0.159077	0.229651	0.334905	0.485044	0.693927	0.979428	1.364162	1.876442	2.551424
6	0.140291	0.195884	0.276794	0.389485	0.542725	0.74767	1.018205	1.37142	1.828188
7	0.123409	0.16691	0.228758	0.312943	0.424911	0.571518	0.761173	1.00406	1.312418
8	0.108242	0.142024	0.188999	0.251543	0.332966	0.437404	0.56987	0.73634	0.94389
9	0.094624	0.120636	0.156052	0.202222	0.2611	0.33513	0.427241	0.540879	0.680069
10	0.082409	0.102247	0.128724	0.162553	0.204849	0.257016	0.320725	0.397925	0.490857
11	0.07147	0.086436	0.10604	0.130615	0.160764	0.197268	0.241054	0.293194	0.354909
12	0.061695	0.072848	0.087204	0.104878	0.126175	0.151509	0.181374	0.216344	0.257063
13	0.052987	0.061184	0.071564	0.084128	0.099013	0.116423	0.13661	0.159867	0.186523
14	0.04526	0.051191	0.058586	0.067398	0.077672	0.089498	0.102996	0.118308	0.135593
15	0.038442	0.042655	0.047836	0.053918	0.060905	0.068827	0.077736	0.087694	0.098773
16	0.032467	0.035398	0.038955	0.043075	0.047743	0.052961	0.058748	0.065127	0.072128
17	0.027281	0.029269	0.031654	0.034382	0.037433	0.0408	0.044486	0.048496	0.05284
18	0.022837	0.024145	0.025696	0.027452	0.029392	0.031509	0.033798	0.036258	0.038891
19	0.019096	0.019922	0.020893	0.021981	0.023171	0.024455	0.025829	0.02729	0.028836
20	0.016025	0.016518	0.017093	0.017732	0.018425	0.019166	0.019951	0.020777	0.021643
21	0.013597	0.013867	0.014179	0.014524	0.014895	0.015289	0.015703	0.016135	0.016585
22	0.011792	0.011918	0.012063	0.012223	0.012393	0.012573	0.012761	0.012955	0.013157
23	0.010596	0.010636	0.010683	0.010733	0.010787	0.010844	0.010903	0.010964	0.011027
24	0.010596	0.010636	0.010683	0.010733	0.010787	0.010844	0.010903	0.010964	0.011027

https://doi.org/10.4314/njt.2026.5351

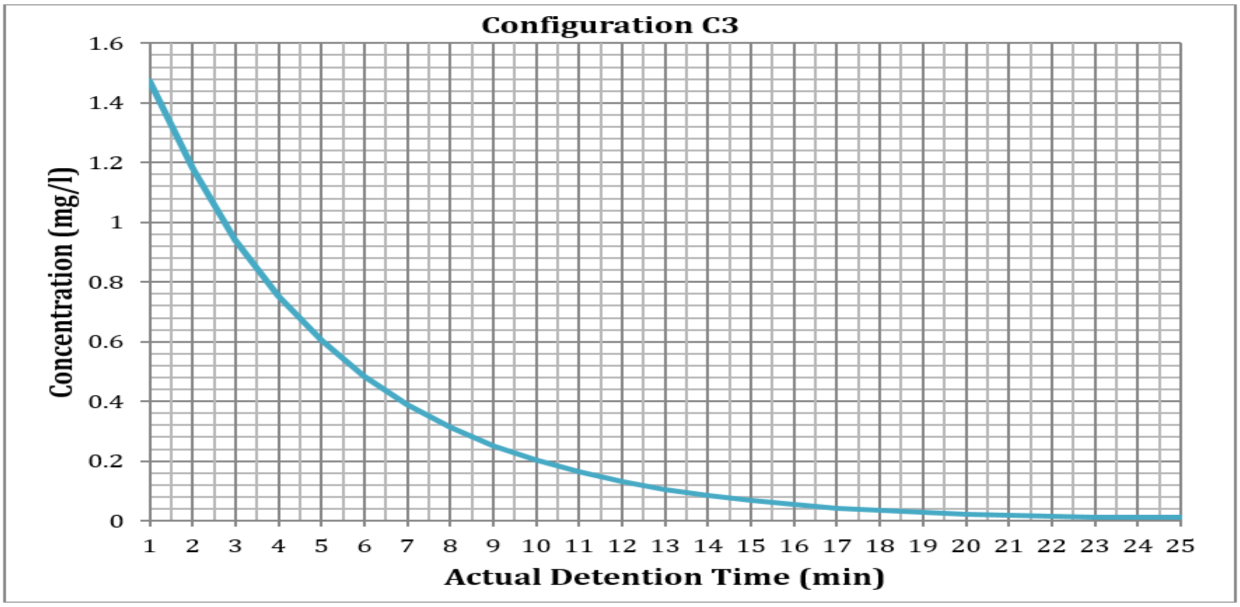

Figure 5: Concentration – time curve for configuration C3, pond length, L = 1.0 m at influent flow rate, Q = 91.6 ml/s

Based on the concentration – time curve presented in Figure 5 above, for a C_e value of 0.104 mg/l, the predicted actual detention time, θ_a was 12.00 min (Experimental θ_a gave 11.33 min). The theoretical detention time, θ_t *was* 18.20 *min*, therefore; Short-circuiting index, α *was determined as* 0.34. Experimental Short-circuiting index, $\alpha = 0.38$.

The flexibility of the model to adjust to the varying pond geometry and flow conditions is due to a well captured initial and boundary conditions in the computational module. Similarly, for the pond with L = 1.5 m, the result is presented in Table 3. The concentration-time curve corresponding to grid 1 of the computational scheme is shown in figure 6.

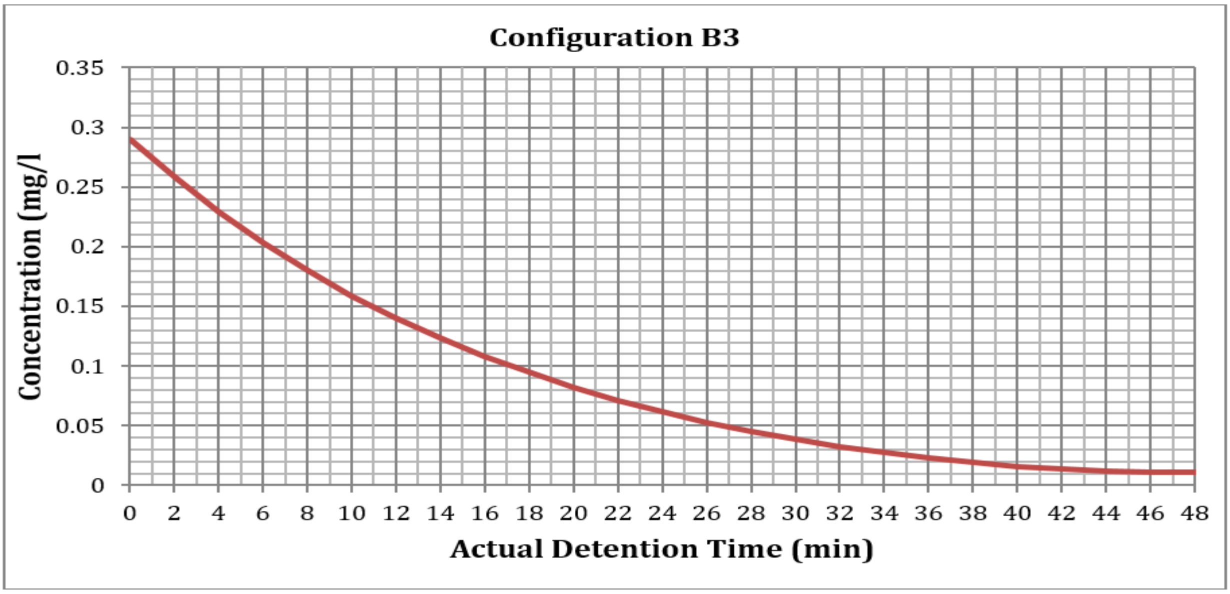

Figure 6: Concentration – time curve for configuration B3, pond length, L = 1.5 m at influent flow rate, Q = 91.6 ml/s

https://doi.org/10.4314/njt.2026.5351

Table 3: Model results for inlet and outlet configuration B3 corresponding to grid 1 for pond length, L = 1.5 m with an influent flow rate, Q = 91.6 ml/s

Time				Effluent	Conc.	(mg/l)			
(min)	Grid 1	Grid 2	Grid 3	Grid 4	Grid 5	Grid 6	Grid 7	Grid 8	Grid 9
0	0.290338	0.50589	0.874865	1.474941	2.419184	3.867652	6.043198	9.252108	13.91065
2	0.258089	0.431926	0.720833	1.177875	1.878828	2.928746	4.470938	6.698547	9.869207
4	0.229187	0.36888	0.594502	0.941925	1.461509	2.221686	3.313973	4.859362	7.016301
6	0.20326	0.315058	0.490712	0.75418	1.138606	1.688187	2.460902	3.531977	4.998164
8	0.179985	0.269044	0.405302	0.604531	0.888301	1.28488	1.830666	2.572034	3.567582
10	0.159077	0.229651	0.334905	0.485044	0.693927	0.979428	1.364162	1.876442	2.551424
12	0.140291	0.195884	0.276794	0.389485	0.542725	0.74767	1.018205	1.37142	1.828188
14	0.123409	0.16691	0.228758	0.312943	0.424911	0.571518	0.761173	1.00406	1.312418
16	0.108242	0.142024	0.188999	0.251543	0.332966	0.437404	0.56987	0.73634	0.94389
18	0.094624	0.120636	0.156052	0.202222	0.2611	0.33513	0.427241	0.540879	0.680069
20	0.082409	0.102247	0.128724	0.162553	0.204849	0.257016	0.320725	0.397925	0.490857
22	0.07147	0.086436	0.10604	0.130615	0.160764	0.197268	0.241054	0.293194	0.354909
24	0.061695	0.072848	0.087204	0.104878	0.126175	0.151509	0.181374	0.216344	0.257063
26	0.052987	0.061184	0.071564	0.084128	0.099013	0.116423	0.13661	0.159867	0.186523
28	0.04526	0.051191	0.058586	0.067398	0.077672	0.089498	0.102996	0.118308	0.135593
30	0.038442	0.042655	0.047836	0.053918	0.060905	0.068827	0.077736	0.087694	0.098773
32	0.032467	0.035398	0.038955	0.043075	0.047743	0.052961	0.058748	0.065127	0.072128
34	0.027281	0.029269	0.031654	0.034382	0.037433	0.0408	0.044486	0.048496	0.05284
36	0.022837	0.024145	0.025696	0.027452	0.029392	0.031509	0.033798	0.036258	0.038891
38	0.019096	0.019922	0.020893	0.021981	0.023171	0.024455	0.025829	0.02729	0.028836
40	0.016025	0.016518	0.017093	0.017732	0.018425	0.019166	0.019951	0.020777	0.021643
42	0.013597	0.013867	0.014179	0.014524	0.014895	0.015289	0.015703	0.016135	0.016585
44	0.011792	0.011918	0.012063	0.012223	0.012393	0.012573	0.012761	0.012955	0.013157
46	0.010596	0.010636	0.010683	0.010733	0.010787	0.010844	0.010903	0.010964	0.011027
48	0.010596	0.010636	0.010683	0.010733	0.010787	0.010844	0.010903	0.010964	0.011027

Based on the concentration – time curve presented in Figure 6 above, considering an effluent concentration of 0.083 mg/l, the predicted actual detention time, θ_a was 20.00 min (Experimental θ_a gave 20.34 min). The theoretical detention time, θ_t *was determined to be* 27.29 *min*, therefore, Short-circuiting index, α *was found to be* 0.27. Experimental Short-circuiting index, $\alpha = 0.25$

Analysis of the result gave a correlation coefficient of 94% and a RMSE of 0.08 for the index.

The summary of the results obtained for a flow rate of 58.8 ml/s for all inlet and outlet configurations and pond lengths; 1.0, 1.5 and 2.0 m are presented in figure 7, 8 and 9 respectively. These results gave an average correlation coefficient of 92% and RMSE of 0.11 when compared with the experimental results.

https://doi.org/10.4314/njt.2026.5351

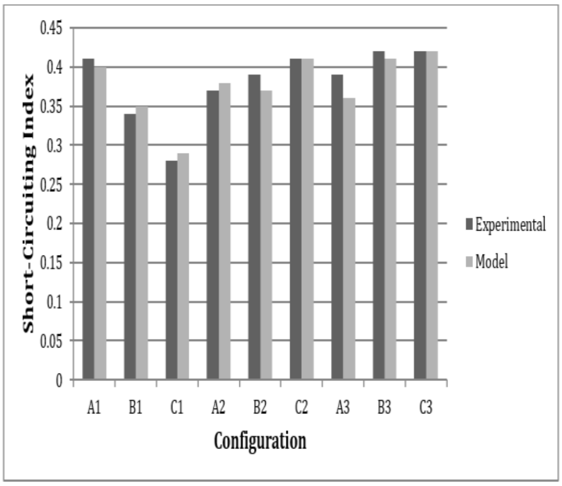

Figure 7: Experimental and model short-circuiting index for pondlength1.0m and flow rate, 58.8ml/s.

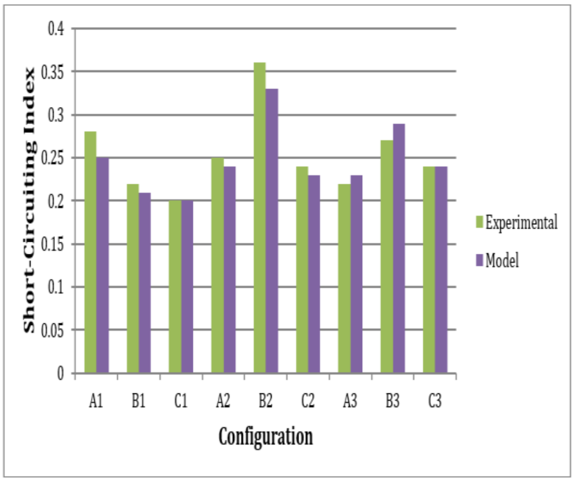

Figure 8: Experimental and Model Short-Circuiting Index for pondlength1.5m and flow rate, 58.8ml/s.

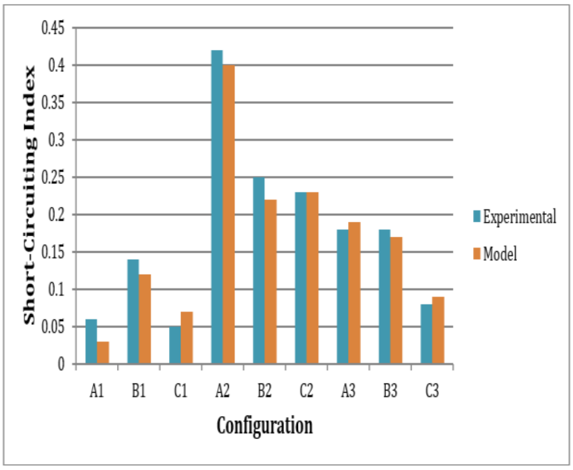

Figure 9: Experimental and Model Short-Circuiting Index for pond length 2.0m and flow rate, 58.8ml/s.

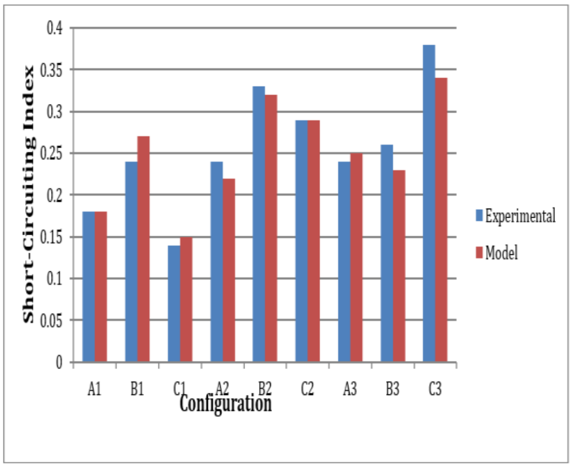

Figure 10: Experimental and model short-circuiting index for pond length; 1.0m and flow rate, 91.6ml/s.

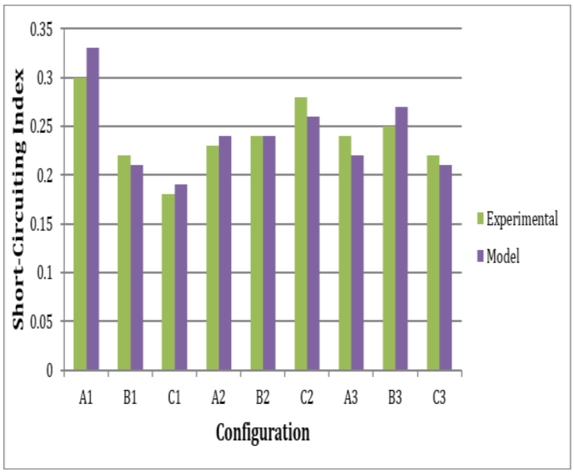

Figure 11: Experimental and Model Short-Circuiting Index forpond length 1.5m and flow rate, 91.6ml/s.

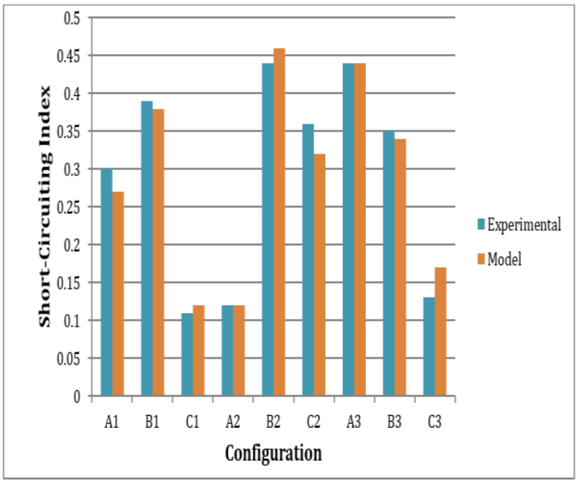

Figure 12: Experimental and model short-circuiting index for pondlength 2.0m and flow rate, 91.6ml/s.

https://doi.org/10.4314/njt.2026.5351

Similarly, the results for a flow rate of 91.6 ml/s for all inlet and outlet configurations and pond lengths; 1.0, 1.5 and 2.0 m are presented in figure 10, 11 and 12 respectively. An average correlation coefficient of 93.5% and RMSE estimate of 0.10 was recorded when compared with the experimental results.

Table 4 shows the summary of results for a flow rate of 120.8 ml/s. An average of 91.8% correlation coefficient was obtained with this data set for the various pond lengths, the average error of estimate, RMSE stood at 0.13.

The negative SCI in Table 4 implies that there is no occurrence of short-circuiting in the pond configuration under review. What it simply means is that the ratio of actual detention time to theoretical detention time is greater than one (1.0). This practically means that the wastewater molecules spend more time in the pond system for the necessary biological processes to take place than it was theoretically designed for. This scenario is similar to having an SCI value of zero (0), which implies no short-circuiting.

Table 4: Summary of experimental values of the short-circuiting Index at different inlet-outlet configurations and lengths, Compared with the model results for a flow rate of 120.8ml/s.

Configuration	Short – Circuiting Index, α Channel Lengths					
	L = 1.0m		L = 1.5m		L = 2.0m	
	Experimental	Model	Experimental	Model	Experimental	Model
A1	0.06	0.02	0.15	0.14	0.40	0.42
B1	0.04	0.05	0.21	0.22	0.34	0.35
C1	0.006	0.00	0.12	0.10	0.14	0.12
A2	0.09	0.07	0.15	0.17	0.15	0.17
B2	-0.13	0.15	0.17	0.17	0.26	0.22
C2	0.14	0.16	0.15	0.12	0.24	0.23
A3	-0.16	0.18	0.23	0.24	0.25	0.25
B3	0.21	0.20	0.15	0.15	0.24	0.21
C3	0.14	0.12	0.23	0.24	0.24	0.26

Based on the numerous pond configurations and the associated flow conditions experimented in this study, it was obvious that SCI is both significantly sensitive to inflow rate as well as pond geometry (length). As a result, design considerations/optimization must take cognizance of both especially with the prevailing circumstances surrounding the scenario. Design optimization in this sense is simply case sensitive, one cannot be said to be more significant than the other.

4.0 CONCLUSION

The short-circuiting index (SCI) is a crucial parameter used to evaluate the hydraulic efficiency of ponds, particularly in wastewater treatment systems. It quantifies the extent to which flow patterns deviate from the ideal plug flow condition, where all water should ideally have an equal retention time within the system.

The SCI helps classify pond hydraulic efficiency in the following ways;

Low short-circuiting index

The lowest SCI in this study was 0.006. A low SCI indicates that water flows uniformly through the pond, meaning that most of the water has an appropriate retention time for treatment. This reflects a high hydraulic efficiency, where the available volume is effectively utilized for the intended treatment processes.

High short-circuiting index

The highest SCI in this study was 0.46 and this suggests significant short-circuiting, where a portion of the inflow bypasses the treatment processes, leading to reduced treatment effectiveness. This can result in inadequate removal of pollutants and suboptimal performance of the system.

https://doi.org/10.4314/njt.2026.5351

Impacts on treatment performance

Systems with a high SCI such as in configuration B2 for an inflow rates of 91.6 ml/s and pond length 2.0 m with SCI of 0.46; may result in poor water quality in the effluent due to insufficient time for biological or chemical processes to occur. Consequently, effluent quality might not meet regulatory standards, necessitating modifications to the design or operation of the pond. Conversely, optimizing pond design systems that do not conform to regulatory standards due to high short-circuiting may be subject to penalties or required upgrades. This can lead to increased operational costs and the need for additional resource allocation to meet compliance.

The model performance

In order to avoid the rigors of redesign or design adjustment, extra costs implications and/or introducing flow control structures such as baffles within the pond, simulating the operation before the actual field construction with the aid of a model offers better alternative and this form the main contribution of this study to existing knowledge. Also, numerous configurations and conditions were modeled in this study, for instance, pond configuration A3 and the associated conditions is a perfect design implication for practitioners to adopt. The accuracy of the model in this study suggests a very good fit. It gave an average correlation of 92.4% with the experimental data with just 0.11 root mean square error of estimate on the average. As shown in the results, SCI value varies with the pond configurations – inlet/outlet placement inclusive. Configurations with low SCI are practically recommended for WSP designers, such includes: A3, B1, C1 etc. See Table 4 and others for guidance. These results are reliable and the model is therefore recommended. However, larger-scale field validation is recommended for future work.

REFERENCES

[1] Agunwamba, J. C. "Field Pond Performance and Design Evaluation Using Physical Models". *Water Research*, 26(10), pp. 1403-1407, 1992. Available at: www.researchgate.net

[2] Agunwamba J. C. "Effect of the Location of the Inlet and Outlet Structures on Short-Circuiting: Experimental Investigation," *Water Environmental Research*, 78, pp. 580-589, 2006. https://doi.org/10.2175/106143006X109603

[3] Bokil, S. Agrawal, G. "Stratification in Laboratory Simulations of Shallow Stabilization Ponds". *Water Research*, II, pp. 1025-1030, 2017. https://doi.org/10.1016/0043-1354(77)90002-1

[4] Danckwerts. P. V. "Continuous Flow Systems". *Chemical Engineering Science*, 2, pp. 1-12, 1953. doi: 10.1016/0009-2509(96)81810-0

[5] Gary, S. K. "Influence of Inlet and Outlet Position on Ponds Hydraulic Short-Circuiting", *Water Resources* 19(3), pp. 297 – 300, 2009. Available at: www.researchgate.net

[6] Marecos do Monte,.M. H. Mara, D. D. "The Hydraulic Performance of Waste Stabilization Ponds in Portugal", *Water Science Technology*, 19(12), pp. 219-227, 1987. Available at: www.waterscience.net

[7] Mangelson, K. A. Waiters, G. Z. "Treatment Efficiency of Waste Stabilization Ponds". *Journal of Society of Civil Engineering*, 98 (2), pp. 407-425, 1972. https://doi.org/10.1061/JSEDAI.0001401

[8] Mara, D. D. Pearson. H. "Artificial Freshwater Environment: Waste Stabilization Ponds. In Biotechnology", *Verlagsgesellschaft: Weinheim, Germany*. 8, pp. 176-205, 1986. Available at: www.scirp.org

[9] Onosakponome O. R, Andy O. I. Anthony. C. E. and Okuroghoboye D. I. "Comparative Analysis of 1-D, 2-D and 3-D Modeling of Waste Stabilization Pond with Computational Fluid Dynamics" *International Journal of Civil Engineering (IJCE)*, 8(6), pp. 20-27, 2021. doi: 10.14445/23488352/IJCE-V8I6P103

https://doi.org/10.4314/njt.2026.5351

[10] Polprasert, C. Bhattarai, K. K. “Dispersion Model for Waste Stabilization Ponds”. *Journal of Environmental Engineering*, 111 (EEI), pp. 45-58, 1985. https://doi.org/10.1061/(ASCE)07733-9372(1985)111:1(45)

[11] Rudra P. “Getting Started with Matlab”. *Oxford University Press, New York*. 2010. Available at: www.scribd.coms

[12] Shilton, A. “Studies into the Hydraulics of Waste Stabilization Ponds”. *Doctorate Thesis,Department of Environmental Engineering*, *Massey University*. New Zealand. 2011. Available at: www.masseyuniversity.org

[13] Onosakponome O. R “Modeling the Effects of Baffles on the Performance of Waste Stabilization Pond Using 3-D Computational Fluid Dynamics”; *International Journal of Engineering, Management and Humanities (IJEMH)*, 2 (4), pp: 74-82, 2023. Available at: www.ijemh.com

[14] Onosakponome O. R, Andy O. I..Anthony C. E. and Odenigbo C “Two-Dimensional Modeling of Waste Stabilization Pond with Computational Fluid Dynamics,” *Saudi Journal of Civil Engineering*, 5(5): pp. 124-132, 2021. doi: 10.36348/sjce.2021.v05i05.004

[15] Onosakponome O. R, Dike B. U and Ukachukwu O. C “Three-Dimensional Modeling of Waste Stabilization Pond with Computational Fluid Dynamics”, *Saudi Journal of Civil Engineering*, 5(9): pp. 367-378, 2022. doi: 10.36348/sjce.2021.v05i09.005

https://doi.org/10.4314/njt.2026.5351